THE ASTROPHYSICAL JOURNAL, 331:699–717, 1988 August 15


# ENCOUNTERS OF DISK/HALO GALAXIES

JOSHUA E. BARNES
Institute for Advanced Study
*Received 1987 December 28; accepted 1988 February 9*

## ABSTRACT

Observations and simplified models have long suggested that disk galaxies interact remarkably often and that some of these systems even merge and perhaps form elliptical galaxies, but detailed numerical evidence on such questions has been slow to accumulate. Here I present the first numerical models of interacting galaxies in which all dynamical components of the participants—bulges, disks, and massive halos—are modeled as fully three-dimensional $N$-body systems with thousands of particles each, and the equations of motion are integrated by a self-consistent algorithm without arbitrary restrictions on the geometry or spatial extent of the mass distribution. Several encounters between multicomponent galaxy models are described, starting with a look-alike for the "Antennae," NGC 4038/9. The influence of massive halos is exhibited by contrasting models run with and without dark matter.

The present study shows that encounters involving pairs of disk/halo galaxies can produce impressive tidal tails while permitting the visible galaxies to merge on a short time scale, mimicking "double-tailed" objects such as NGC 7252. It turns out that extensive dark halos are very effective at soaking up binding energy and angular momentum from other components, significantly altering the distribution and dynamics of the luminous material. The collisions of model disk/halo galaxies described here produce slowly rotating remnants with surface brightness profiles approximating de Vaucouleurs law. The effective radii, shapes, and velocity dispersions of these remnants are generally consistent with elliptical galaxies.

*Subject headings:* galaxies: evolution — galaxies: interactions — galaxies: structure

## I. INTRODUCTION

That tidal interactions between disk galaxies can account for many of the structures seen in peculiar galaxies was argued most convincingly by Toomre and Toomre (1972, hereafter TT; see also Wright 1972; Eneev, Kozlov, and Sunyaev 1973), who modeled encounters between disk galaxies using a restricted three-body approximation. Simple though these calculations were, they showed that remarkably elongated features can be produced by the purely kinematic response of a rotating disk of stars to a sudden tidal perturbation. Furthermore, TT fit the separate responses of individual galaxies together to obtain reconstructions of four well-known objects. This research led to many further questions concerning the formation of eccentric bound pairs, their subsequent orbital decay, the relation of tidal interaction to grand-design spiral structures, and the ultimate fate of interacting pairs. TT recognized that such questions demanded a fully self-consistent dynamical treatment, and called for "proper $N$-body calculations," in which all particles attract each other, to supplement their simplified models.

In the years following TT's publication, several lines of evidence developed pointing to extended, massive dark halos around individual disk galaxies and in pairs and larger systems of galaxies (see Faber and Gallagher 1979). This evidence prompted a sweeping reinterpretation of galactic and extragalactic dynamics and provided a unifying hypothesis for theories of galaxy formation. Although TT had sometimes softened the gravitational potential to imitate slightly extended mass distributions, they were not then motivated to consider interactions of galaxies embedded in massive dark halos, such as those envisioned in the dark matter cosmogony of White and Rees (1977). As White (1982) emphasized, a proper treatment of this more realistic case again requires a self-consistent model to calculate correctly the behavior of the halo distribution.

Proper $N$-body calculations modeling the interaction of "hot" (pressure supported) stellar systems were undertaken by van Albada and van Gorkom (1977), White (1978, 1979), Miller and Smith (1980), Villumsen (1982), Farouki, Shapiro, and Duncan (1983), and Aguilar and White (1985, 1986), among others. These experiments exhibited a number of interesting results, including tidal friction between interacting systems and consequent orbital decay, spin-orbit coupling in the interaction of hot, rotating systems, partial mixing of radial gradients in merging encounters, nonhomology of merger remnants with respect to progenitors, and generic density profiles changing from $\rho \propto r^{-3}$ in the body of the remnant to $r^{-4}$ at large $r$ due to particles near escape energy. But because they treated hot systems, these specific calculations are directly relevant only to interactions of ellipticals and perhaps to encounters of dark halos surrounding visible galaxies.

Self-consistent models of "cold" (rotation supported) systems in interaction were attempted by Gerhard (1981), Farouki and Shapiro (1981), Quinn (1982), and Negroponte and White (1983). These calculations proved much more difficult than those involving hot systems, essentially because a cold, self-gravitating disk of particles is so remarkably sensitive to $\sqrt{N}$ fluctuations. Disk galaxies modeled with only $\sim 10^3$ particles forget much of their initial structure in a few crossing times; to correct this problem, there is really no substitute for drastically increasing $N$.

As a consequence of these numerical difficulties, several interesting questions about encounters of disk/halo galaxies have not been convincingly resolved to this date. One question, stressed by Toomre (1977), is whether "two disk systems in

some ... grazing passage necessary to produce impressive tails can actually stop and merge rapidly enough" to explain galaxies such as NGC 7252, where a pair of prominent, dynamically young tails extend from a single ellipsoidal object. Can massive dark halos really provide sufficient dynamical friction to bring the two galaxies to the screeching halt that seems to be required? Another question concerns the binding energy of merger remnants: Ostriker (1980) argued that the merger of disk galaxies from parabolic orbits would produce diffuse, low-velocity dispersion remnants inconsistent with real elliptical galaxies. Can the halos of merging galaxies absorb the excess binding energy? A third question pertains to the angular momenta of merger remnants; White (1979) found that off-axis mergers of spherical galaxies usually result in oblate objects rotating too fast to resemble bright ellipticals. Can halos likewise absorb the angular momentum?

These three important questions are all essentially in the domain of stellar dynamics, trivially extended to include the presumably collisionless dynamics of the dark matter. Other outstanding problems, such as the origin of radial gradients (White 1980) and the maximum phase space density of merger remnants (Carlberg 1986), may very well involve the messy and highly uncertain physics of star formation. Nevertheless, purely stellar dynamical calculations provide a baseline from which more comprehensive models can be developed.

In this work, I simulate interacting disk/halo galaxies using an $N$-body algorithm recently developed by Barnes and Hut (1986) which combines the favorable scaling of potential solving methods with the generality and simplicity of direct summation codes. Extensive numerical tests by Hernquist (1987) and Barnes and Hut (1988) show that this "tree code" is well suited to problems involving the essentially collisionless evolution of large-$N$ systems over a modest number of crossing times. This algorithm makes it possible to run enough particles ($\sim 10^4$ per galaxy) to model the overall behavior of disk galaxies reasonably well without imposing artificial restrictions on the symmetry or physical extent of the interacting systems. Thus the present calculations represent a significant advance over previous efforts, extending $N$-body simulation techniques to fairly realistic models of interacting galaxies. The dynamical effects now revealed clearly by such models may someday inspire a systematic survey of galactic collisions, but such an undertaking is still some time off; the major technical obstacles at this time concern the generation of initial conditions and the reduction of the results. This study is a first look at the new terrain, exposing some of the more striking phenomena found in interactions of disk galaxies, but not covering the ground in detail. In particular, I focus here on the three outstanding stellar dynamical problems raised above.

The plan of this paper is as follows. Section II presents a model for the "Antennae" and compares it to observations. Section III describes a small selection of interacting disk galaxy models, discusses the forms of orbital decay seen in these models, and presents the transfer of angular momentum as an example of galaxy-halo coupling. Section IV reports on the overall structure and dynamics of a merger remnant. Discussion and conclusions appear in § V. Three appendices give the technical details for the initial conditions used in these encounter simulations. Appendix A describes the construction of model galaxies: self-consistent $N$-body methods are used to bring the spheroidal components into equilibrium, while the disks are generated from an assumed density distribution and given an approximately consistent rotation velocity. Tests of several such models are presented in Appendix B; these show that the construction procedure yields near-equilibrium initial data, and that the models are stable enough for the present application. The generation of initial conditions for the simulated encounters is discussed in Appendix C.

## II. AN NGC 4038/9 LOOK-ALIKE

As a warmup exercise in the best $N$-body tradition, I constructed a model of the well-known "Antennae," NGC 4038/9. The initial conditions correspond closely to the model by TT, although the inclusion of massive dark halos requires some modification of their prescription. I used prototype bulge/disk/halo galaxy models similar to model 1 described in Appendix A: mass ratio of components 1:3:16, total mass $M_B + M_D + M_H = 1.25$, exponential disk with inverse scale length $\alpha = 12$, circular orbital period $t_{\rm orbit} \approx 0.93$ at radius $r = 3/\alpha$, with all quantities measured in arbitrary units with $G = 1$. Scaling these numbers roughly to our own Galaxy, the units of length, time, and mass are 40 kpc, 250 Myr, and $2.2 \times 10^{11}$ $M_\odot$, respectively. The galaxies were started on elliptical orbits with eccentricity $e = 0.5$, pericentric separation $r_p = 0.5$, and time to pericenter $t_p = 1$. Following TT, both galaxies were inclined by $i = 60°$ to the orbital plane, with pericentric arguments $\omega = -30°$. These initial conditions are chosen to produce a slow and symmetrically prograde encounter, with the two disks inclined so as to sling tidal tails high above the orbital plane where they will eventually be seen in projection as crossing each other. A schematic of this setup appears in Figure 1.

Since the model galaxies used here are extended systems with many internal degrees of freedom, the encounter of two such objects would hardly be expected to follow the behavior of TT's quasi-Keplerian model for very long. In fact, the tidal coupling of orbital to internal motion is so efficient in this self-consistent model with massive dark halos that its relative orbit decays in less than one initial orbital period. At the time when TT's model most closely matches the observations, the galaxies in the present model have already merged. Nevertheless, the self-consistent calculation does produce a configuration bearing a fair resemblance to 4038/9 when viewed from the direction suggested by TT, albeit at a considerably earlier time: $t = 1.8$, or roughly one-fourth of an initial orbital period after pericenter. This subjectively chosen "best fit" may be seen in Figure 2; a time sequence using color to distinguish the bulge, disk, and halo components appears in Hut and Sussman (1987).

Other views of this configuration are presented in Figure 3. The first three frames compare the distributions of bulge stars, disk stars, and dark mass, respectively, as projected on the orbital plane of the system. Note the clean separation of the two bulges in Figure 3*a* in contrast to the complex patterns traced by the disk stars in Figure 3*b*. Detailed measurements confirm that the interaction has slewed the inner galactic disks by $\sim 70°$ counterclockwise, almost edge-on to the line of sight; evidently powerful torques were applied to the disks during the encounter. The halo distribution in Figure 3*c* broadly follows the luminous material, like a dark, distended body surrounding a luminous spine. Distinct peaks in the dark mass distribution which coincide with the luminous nuclei may be lost in the reproduction. That the visible tails do not protrude from the halo is perhaps not completely surprising since a small fraction of that dark mass must initially have shared phase space with the luminous stuff, and thus "tags along" to the present.

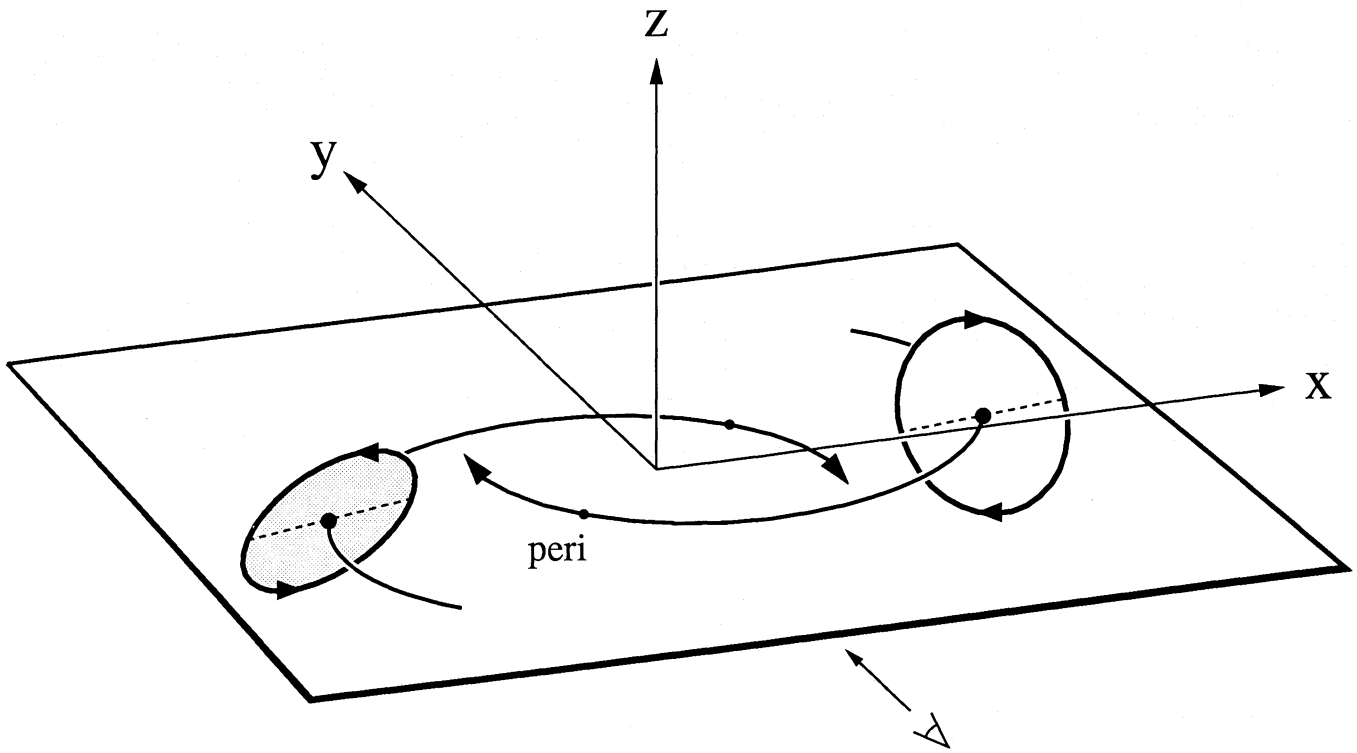


FIG. 1.—Geometry of the initial orbit for the NGC 4038/9 look-alike. The two disks are shown at their starting positions, one time unit before pericenter. They are symmetrically inclined by 60° to the orbital plane; dashed lines show where the disks intersect the orbital plane. Viewing direction for Fig. 2 is shown by the arrow.

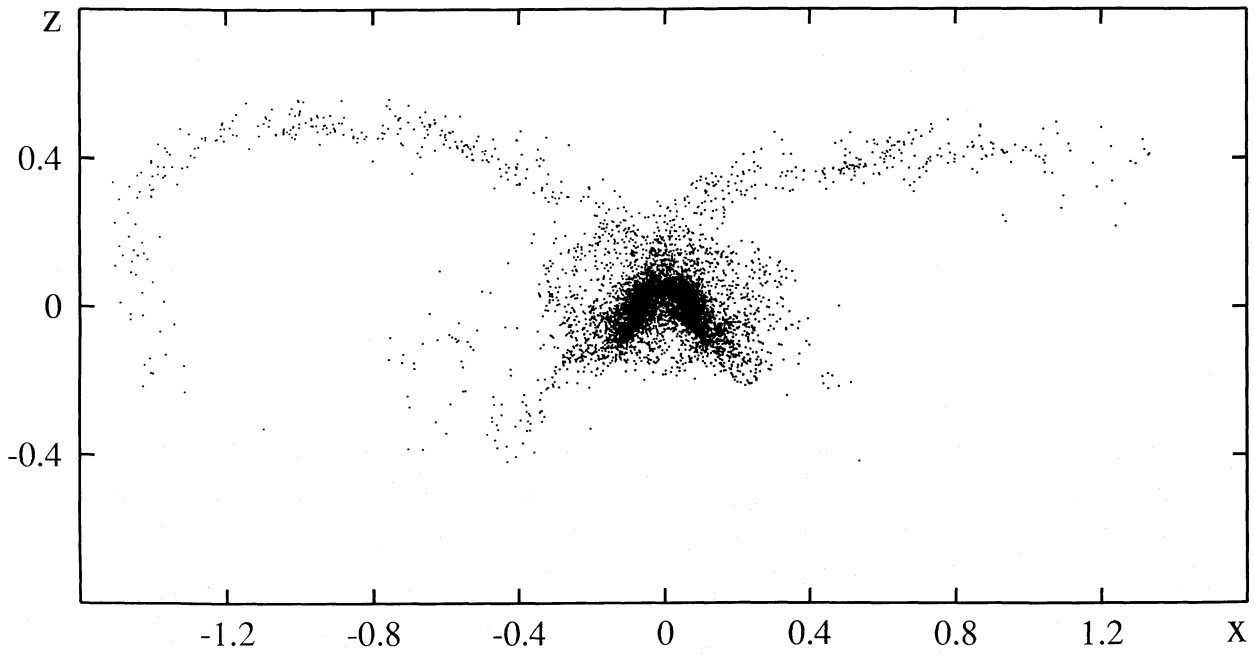


FIG. 2.—NGC 4038/9 look-alike. This configuration was produced by an encounter of two bulge/disk/halo galaxies on an $e = 0.5$ orbit. The view is edge-on to the orbital plane; only luminous (bulge + disk) components are plotted.

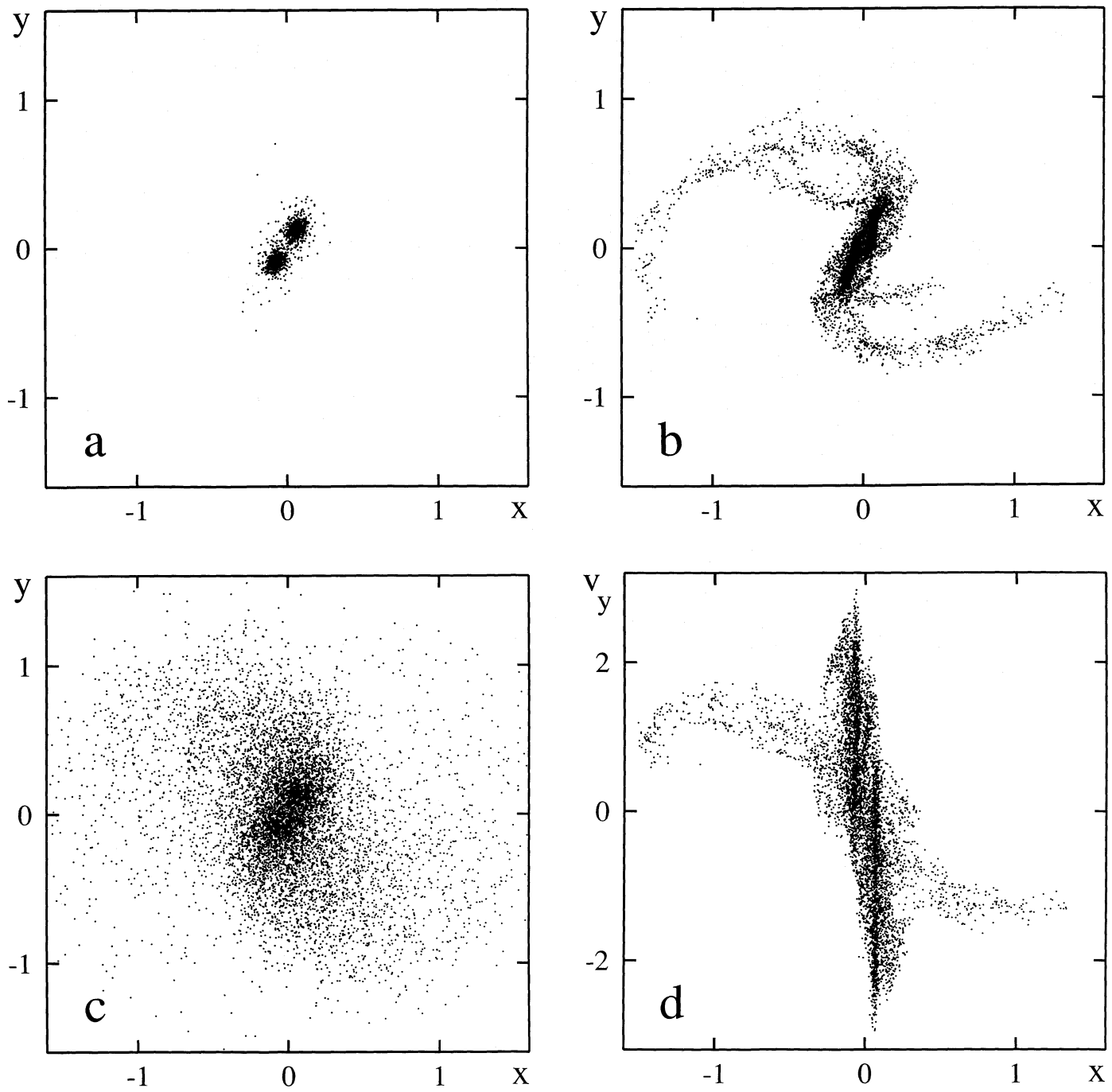


FIG. 3.—Additional views of the NGC 4038/9 look-alike at the instant shown in Fig. 2. Distributions of the (*a*) bulge, (*b*) disk, and (*c*) halo, respectively, projected onto the orbital plane; the galaxies move clockwise. (*d*) Line-of-sight disk particle velocities plotted vs. position along the line defined by the intersection of the sky and orbital planes.

Incidentally, the more curving left-hand tail of this model matches rather closely the appearance of the SW tail of 4038/9 as seen in deep optical images by Schweizer (1978; see also Zwicky 1959), and also in the high-resolution H I map of Mahoney, van der Hulst, and Burke (1987). This asymmetry between the two tails, which seems such a convincing feature of the calculation, is *not* due to any macroscopic asymmetry in the initial conditions. It resulted instead from $\sqrt{N}$ fluctuations in the galaxies, which happened to be swing-amplified by the disk and sheared out by tidal forces at encounter so as to further populate one of the resulting tidal arms.

Serendipitous asymmetry aside, what are the real successes and failures of this calculation? One favorable point is the narrowness of the tidal tails, showing that the care taken here to insure that the disks are still relatively cold at encounter has paid off; compare the very thin tails produced by TT's cold test-particle calculations with the rather thick, stubby tails of Negroponte's (1982) self-consistent model shown in Figure 4 of

White (1982). From some projections, the present tails even have the appearance of thin, ribbon-like surfaces as suggested by TT, although this is hard to verify since these tails are not very densely populated. A second favorable point is the proximity of the main bodies of the two galaxies, a distinct improvement on the idealized model of TT. As those authors foresaw, this improvement can be credited to the decay of the initial elliptical orbit due to tidal friction. Yet even they scarcely anticipated the strength of this effect: our two bulges, which track the dynamical centers of the galaxies, barely separate after pericenter, and plunge back together after roughly one-third of an orbital revolution.

Indeed, the two galaxies are shown here just before their second encounter, which would be in splendid agreement with TT's suggestion that 4038/9 "are about to do it again" but for one catch. The model galaxies in Figure 2 are approaching each other almost along the line of sight, with a projected velocity comparable to the circular velocity of each individual disk. This is illustrated in Figure 3*d*, where the line-of-sight velocity of each disk particle is plotted versus position along the intersection of the sky and orbital planes. Yet Rubin, Ford, and D'Odorico (1970) found H II velocities differing by only 38 km $s^{-1}$ for the nuclei of 4038 and 4039 (knots J+K and A in their notation). Interpretation of these observations is made difficult by the partial overlap of these dusty galaxies, but the recent H I study by Mahoney *et al.* also indicates a small line-of-sight velocity difference for 4038/9. Thus the present model, although in many respects an improvement over previous ones, still fails to match the observed kinematics of the main hulks of 4038/9.

This model may also be criticized on more theoretical grounds: how could this relatively short-period $e = 0.5$ orbit have come about? Assuming that the two galaxies were originally on a long $e \approx 1$ relative orbit, one might conceivably appeal to a previous passage as having left the two actors on the course leading to their recent collision. However, to avoid preemptively inflicting the damage responsible for the present tails, the hypothesized previous passage must have been much wider; one must then invoke dynamical friction to produce a considerably closer encounter the second time around. This requirement would perhaps be met if the galaxies were embedded in very extensive dark halos which could generate dynamical friction not just at pericenter but throughout the previous passage, favoring decay of the pericentric distance $r_p$.

Alternatively, it may be that the last and only incoming orbit was considerably more eccentric than our assumed $e = 0.5$. A modest increase in $e$ would probably help delay the final plunge of the two galaxies and thereby lessen the observational criticism above. However, the close parabolic encounters about to be described do not easily produce configurations with crossed tails like the Antennae, essentially because the galaxies separate in the same direction that their tails do.

## III. A MODEST SURVEY OF PARABOLIC ENCOUNTERS

Encouraged by the qualified success of the model for the Antennae described above, I began a series of experiments to obtain some feeling for the space of possible encounters. Experience with these calculations led to the selection of the following four encounters as good (if sometimes extreme) examples of behavior relevant to the outstanding stellar dynamical questions raised in § I. The focus on close passages in this selection reflects an inevitable compromise between ambition and finite computer resources. Wider passages, which are probably more common, would have exhibited subtler effects and taken longer to run to ultimate merger or eventual escape; both factors make their study more expensive.

Parameters for the four chosen encounters are summarized in Table 1; Appendix C describes how the initial conditions were generated. To exhibit the major effects of dark halos, collisions were set up between similar pairs of galaxies with luminous/dark mass ratios of 1:0, 1:4, and 1:8 in encounters 0, 1, and 2, respectively. The incoming galaxies were assumed to fall from rest at infinity, producing parabolic passages; this is in keeping with TT's hypothesis that most interacting galaxies were until recently bound in *very* eccentric orbits with periods of roughly the Hubble time $H_0^{-1}$, and are only now experiencing their first collision. A pericentric separation of $r_p = 0.2$ was chosen for the incoming parabolic orbit, producing a relatively close passage. The two galaxies were assigned the same orientations with respect to each other and to the orbit as in the model for the Antennae: $i_1 = i_2 = 60°$, $\omega_1 = \omega_2 = -30°$, except for encounter 1R with reversed spins, $i_1 = i_2 = -120°$. However, in all four of these encounters, the separation vector at pericenter was aligned parallel to the $x$-axis, rather than at an angle of 45° as seen in Figure 1.

A total of $N = 16{,}384$ particles was used in each case; forces were calculated via a tree algorithm modified to include quadrupole moments in cell interactions, with critical opening angle $\theta = 1$ and softening length $\epsilon = 0.015$; particles were advanced by a time-centered leapfrog with $\Delta t = 1/128$. Energy and angular momentum were conserved to within 1% which seems sufficient for the job at hand. Running an F77 implementation of the tree code developed by L. Hernquist, which I modified to use only standard iterative control structures, each unit of model time required ~75 minutes of Cyber205 CPU time. The survey described here took ~25 hr in total. To check that numerical errors do not compromise the results, encounter 1 was repeated with smaller values for the time step $\Delta t = 1/256$ and opening angle $\theta = 0.7$, conserving $E$ and $J_z$ to $-2 \times 10^{-3}$ and $\sim 10^{-3}$, respectively. The improved calculation produced results very similar macroscopically to the original run, although details of the particle distribution were of course different.

### a) *Formation of Tidal Tails*

Snapshots of these four calculations, taken 0.5 time units after the first passage, are shown in Figure 4; the orbital plane is viewed face-on. Of these four examples, the two which most closely resemble each other are the standard-halo and double-halo models in Figures 4*a* and 4*b*; the latter merely shows the

TABLE 1

PARABOLIC ENCOUNTERS

| Identification | Galaxy | *B*:*D*:*H* | $r_p$ | $t_p$ | $i$ | $\omega$ |
|---|---|---|---|---|---|---|
| 1 ..... | 1 | 1:3:16 | 0.2 | 1.0 | 60° | −30° |
| 2 ..... | 2 | 1:3:32 | 0.2 | 1.0 | 60° | −30° |
| 0 ..... | 0 | 1:1:0 | 0.2 | 1.5 | 60° | −30° |
| 1R ..... | 1 | 1:3:16 | 0.2 | 1.0 | −120° | −30° |

NOTES.—All encounters involve similar, equal-mass galaxies; B:D:H is the ratio of bulge, disk, and halo components by mass; all encounters are parabolic, with targeted pericentric separation $r_p$; $t_p$ is the time until pericenter; $i = i_1 = i_2$ is the inclination of the galactic disks to the orbital plane, and $\omega = \omega_1 = \omega_2$ is the pericentric argument.

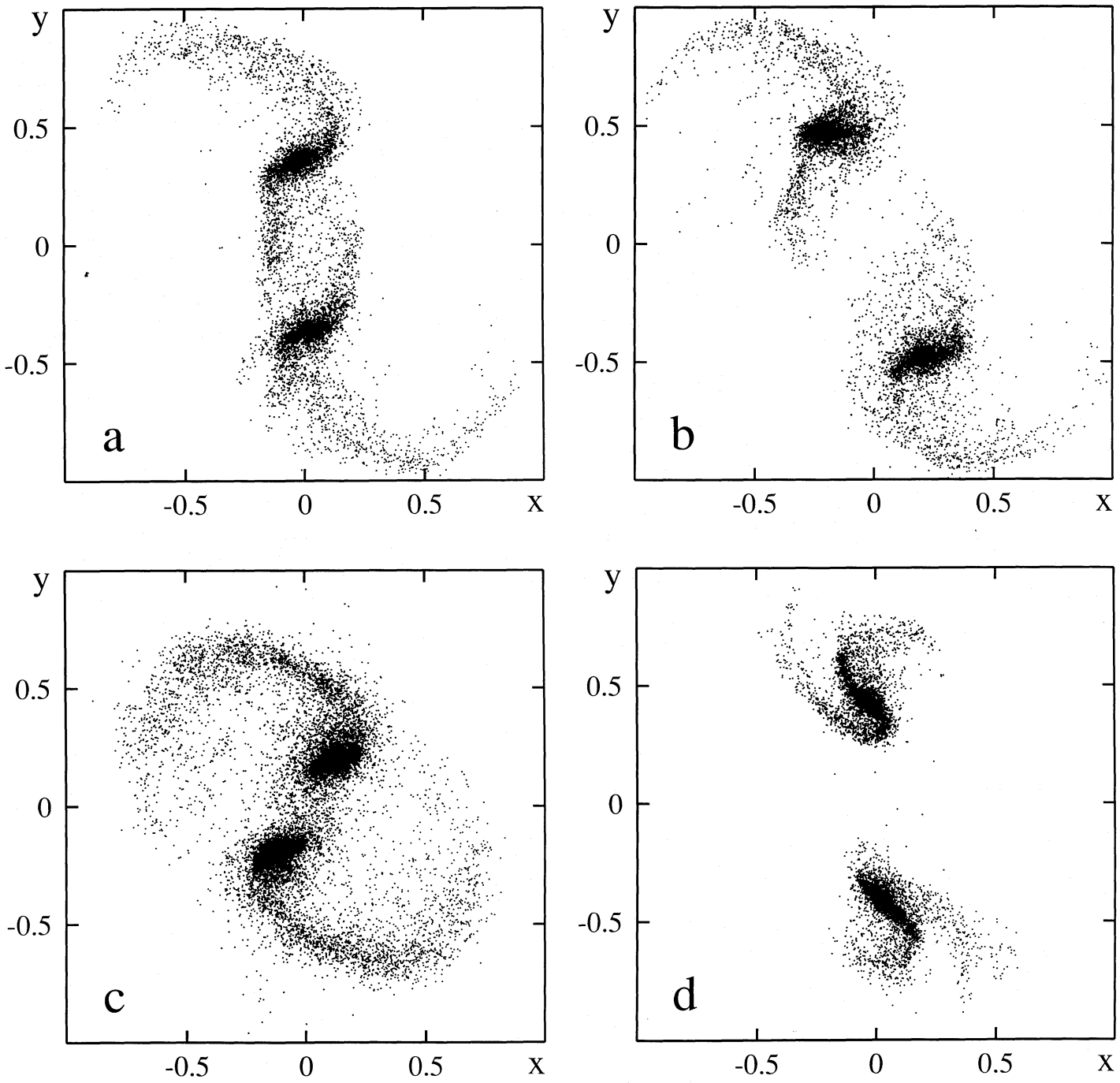


FIG. 4.—Four parabolic encounters, all 0.5 time units after pericenter. These views are face-on to the orbital plane, with galaxies moving clockwise about each other; only the luminous components are plotted. Equivalent prograde encounters 1, 2, and 0 of similar galaxies with (*a*) standard halo, (*b*) extra halo, and (*c*) no halo mass, respectively. (*d*) Encounter 1R, a retrograde version of encounter 1.

results of an encounter somewhat faster than the former, the extra halo mass around these double-weight galaxies having deepened their potential wells. In contrast, the encounter involving halo-free galaxies in Figure 4*c* yields very different results: much of the disk material gets stripped from the galaxies and travels outward in two sweeping counterarms. Without the dark mass to accelerate them to higher speed at pericenter, these galaxies suffer more violent encounters, as their extensive tidal damage attests. Finally, contrast all these encounters (and especially the first one) with the spin-reversed $i = -120°$ encounter 1R shown in Figure 4*d*. Retrograde encounters clearly make less of a splash than prograde ones, yet here, too, tidal arms wind away from each galaxy. These arms seem distinctly more striking than those produced in fully retrograde encounters of test particle disks (e.g., TT Figs. 1, 7), suggesting once again that self-gravity boosts the response of a disk to tidal perturbations (Toomre 1981). A recent study by Noguchi (1987), using a two-dimensional FFT code with a

rigid halo potential, nicely illustrates this point. Careful examination of results from the present calculations also supports Noguchi's major claim that otherwise stable galaxies subjected to a strong tidal perturbation can develop striking if temporary bars.

The same four models are shown 2 time units after pericenter in Figure 5. By now, two of the four pairs have merged; the other two still exhibit distinct nuclei, which are, however, in close interaction and will soon merge. All three halo-galaxy encounters have left extended tails, although only in the prograde cases will these tails actually escape to infinity. Encounter 0, lacking a halo component, is unusual. The slow passage of these galaxies has stripped off much of the disk mass, with ~30% unbound. The fat, sweeping arms which result are unlike most of the narrow tails pictured by Arp (1966).

The ease with which encounters involving halo galaxies produce tidal tails is somewhat surprising. White (1982) worried that if galaxies are embedded in massive halos, "the relative velocities of the two galaxies at pericenter will be increased [and] in addition the tails will need to climb out of a

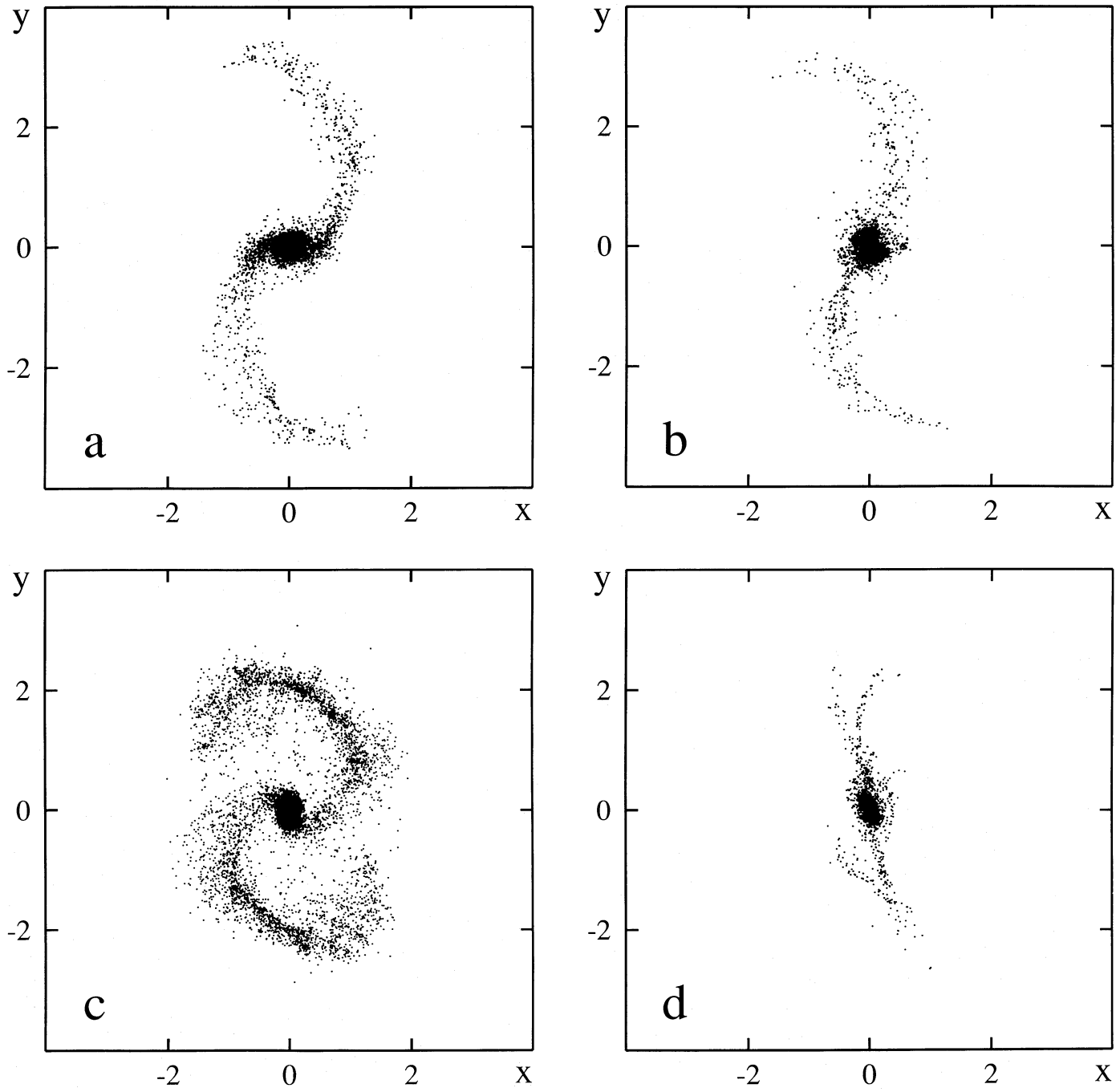


FIG. 5.—Further evolution of parabolic encounters. Viewing angle, and so on, are as for Fig. 4, but field of view has expanded to take in the extended tails. The two left-hand systems have just merged, while the two on the right are in the throes of their final encounter.

deeper potential well .... Both these effects must make it more difficult to model the long tails seen in some observed systems." The first effect is certainly seen in the present calculations: in encounters 0, 1, and 2, the galaxies fly past each other with approximate velocities of 2.2, 4.0, and 4.6, respectively, with less damage in the latter cases. However, the second "effect" does not significantly influence the length of the tails, since the energy needed to climb out is actually provided by falling in. At pericenter when the tidal fields are strongest, material on the far sides of the interacting galaxies shears away—or gets left behind—on more nearly linear trajectories. This material, destined to form the extended tails, retains much of the velocity acquired on the way down, plus a contribution from internal motion in prograde cases. With perhaps a little help from the self-gravity of their disks to amplify the tidal response, the disk/halo galaxy encounters studied here have no trouble in producing well-developed tails.

### b) *Modes of Orbital Decay*

A general difference between collisions involving galaxies with and without dark halos is illustrated by Figure 6, where trajectories of the central bulges in encounters 1 and 0 are compared with extrapolations of the incoming parabolic trajectories. As already noted above, the dark halos in effect boost the infalling visible galaxies to mildly hyperbolic speeds at closest approach; thus in encounter 1 the two galaxies turn wide of the track. The massive halos surrounding these galaxies, being so extended, suffer a more nearly head-on collision, and their collective response produces a large temporary concentration of dark mass that lags behind the visible galaxies. It is the gravitational field of the combined halos which practically stops the outgoing galaxies in their tracks and returns them so soon for further processing. This decay mechanism is seen in all three halo-galaxy calculations; even reversing the galactic spins as in encounter 1R has little overall effect.

Without dark halos the encounter goes very differently: after they pass each other, the galaxies then "fall off" on the inside of the parabolic track, and eventually spiral together. The relatively slow passage of these galaxies and the intrinsic wave amplification in their relatively massive disks combine to produce a huge tidal response, and this in turn provides the dynamical friction which brings them back together. This decay mechanism is probably very spin dependent (White 1979); further simulations may eventually establish whether disk galaxies can ever *gain* orbital energy in an encounter as suggested by TT (n.9) and by Palmer and Papaloizou (1982).

### c) *Transport of Angular Momentum*

The orbital decay discussed in the last two paragraphs may be largely understood as the result of transfer of binding energy and angular momentum from the two bulges to more outlying parts of the system. A quantitative discussion of energy transfer in a multicomponent $N$-body system is complicated inasmuch as we cannot rigorously define the total binding energy of a finite component; kinetic and potential terms must be treated separately. On the other hand, the total angular momentum of a fixed Lagrangian volume, computed with respect to the center of mass, is well defined and remains constant for axisymmetric systems. By effectively including both orbital motion and internal spin contributions, it isolates the effects of transport to other components.

Since the bulges used in these simulations are initially nonrotating, the total angular momentum of the bulge components, $\boldsymbol{J}_B$, starts parallel to the orbital ($z$) axis, and remains approximately parallel throughout the calculation. Figures 7*a* and 7*b* show the $z$ component of $\boldsymbol{J}_B$ as a function of time in encounters 1 and 0, respectively. Results are plotted for both versions of encounter 1, which represent the same physical situation but used different "microscopic" initial conditions, force calculation tolerance, and time step.

Comparing the two realizations of encounter 1, we see that the net angular momenta of the bulges fluctuate at early times, while later on the agreement between the two calculations becomes much better. These early fluctuations seem due to transient spiral features in the surrounding disks, further described in Appendix B, which exchange linear momentum with the bulges. As the two galaxies draw nearer, these exchanges have less effect on $\boldsymbol{J}_B$, since the lever arm decreases. The strongest torques act on the bulges at $t \approx 1.3$, shortly after first passage. At this time, the dark halos have been compressed by their gravitational interaction, and lag somewhat behind the luminous bulges in orbital phase, providing a highly effective drag on the bulges. After their eventual merger a $t \approx 2.5$, the total angular momentum content of these two bulges has fallen by the remarkably large factor of $\sim 25$.

Much less transport of angular momentum occurs in the collision of galaxies without massive halos, as seen in encounter 0. Here the bulges comprise half the total system mass, and transient spirals in the surrounding disks have less effect than in encounter 1. After first passage at $t \approx 1.5$ and before $t \approx 2$, the bulges lose some of their angular momentum to the massive trailing counterarms, but the net coupling is small and even changes sign once the phase lag between the bulges and counterarms exceeds 90°. The net loss of angular momentum suffered by these bulges comes to a mere factor of $\sim 1.7$.

## IV. POSTMORTEM OF A MERGER REMNANT

The possibility of making elliptical galaxies by bashing spirals together has inspired several authors to examine merger remnants in numerical (e.g., Gerhard 1981; Negroponte and White 1983) and observational (e.g., Schweizer 1982; Lake and Dressler 1986) studies. The numerical results have been complicated by spurious relaxation, which makes the incoming disks "puff up" vertically in a few dynamical times. While we can solve this problem by pushing $N$ up until the continuum limit is identified, such an approach is still somewhat extravagant. With more than 10 times as many particles, however, the present models are less afflicted by two-body relaxation than those cited above, so it is interesting to examine the remants produced in these calculations. Here I focus exclusively on the remnant produced by encounter 1, deferring a comparative study of remnant morphology until relaxation is still better controlled.

The spatial and phase space structure of this remnant, recorded at time $t = 4$, is shown by Figures 8 and 9, respectively. Figures 8*a–c* present orthogonal closeups of the remnant and surrounding material; Figure 8*d* offers a large-scale view, to be discussed shortly. The system is dominated by a dense central ellipsoid, with axes approximately in ratio 6:7:10, which originated in a final, nearly head-on collision of the surviving bulges of the incident galaxies at time $t \approx 2.5$. The joint distribution of bulge stars in radius $r$ and radial velocity $v_r$ is shown in Figure 9*a*. At $t = 4$ this plot looks remarkably symmetric with respect to the $v_r = 0$ axis and reveals little fine-grain structure, suggesting that the central ellipsoid has already reached an approximate dynamical equi-

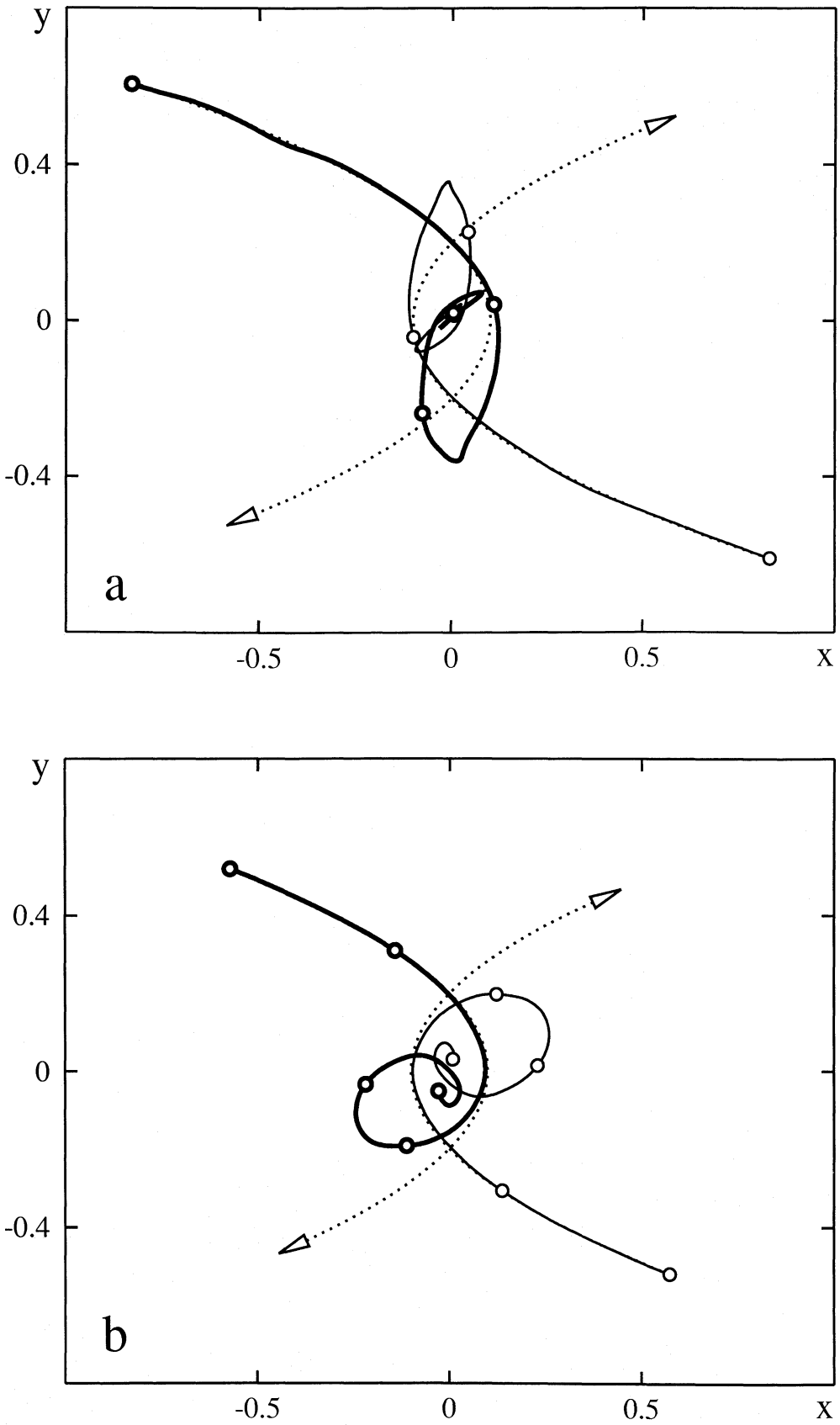


FIG. 6.—Orbital trajectories of the central bulges in encounters 1 and 0, shown in (*a*) and (*b*), respectively, illustrating orbital decay with and without dark halos. Circles indicate positions at unit time intervals. Also shown are the parabolic trajectories which the galaxies would follow if they were point masses (*dotted*).

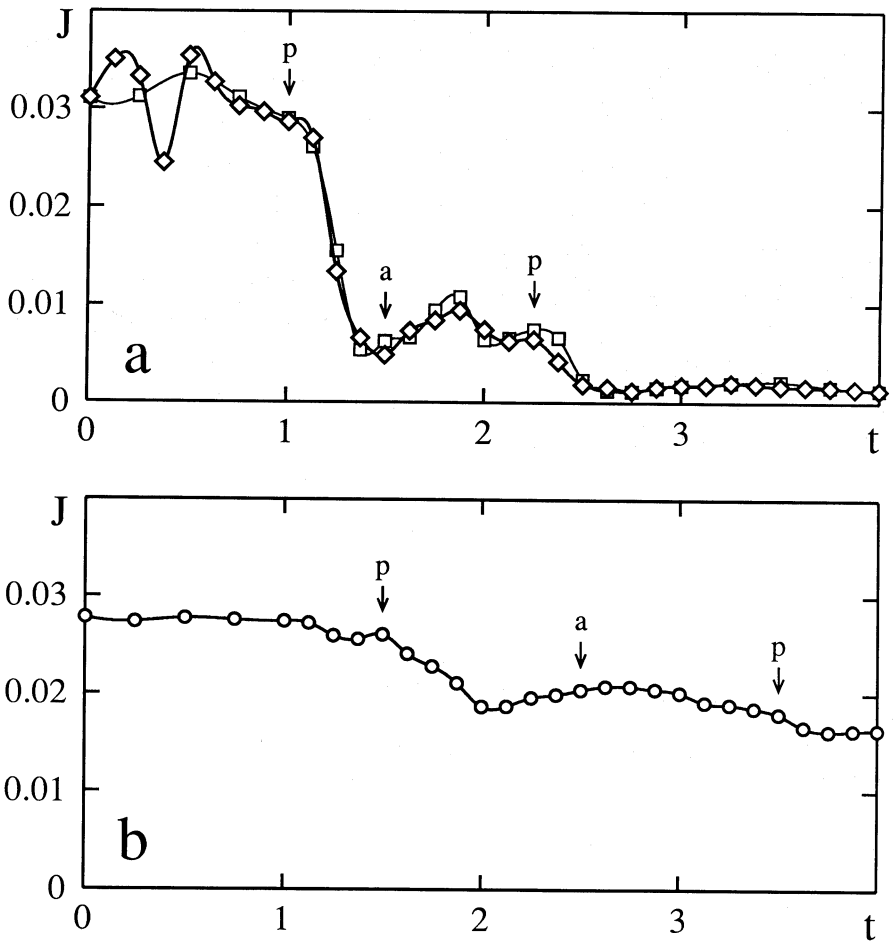


FIG. 7.—Decay of orbital angular momentum stored in the bulge components during merging encounters of galaxies with and without dark halos. First pericenter, apocenter, and second pericenter occur at the times indicated. (*a*) Results for both versions of encounter 1, with the more accurate calculation plotted with diamonds. Note the rapid transfer of angular momentum shortly after first encounter, typical in disk/halo galaxy encounters. (*b*) Results for encounter 0, in which no dark component was present; following first passage only a little angular momentum is lost.

librium. Stars originally in the inner third of the incident disks show a similar but slightly more extended distribution. The prolate form of this central ellipsoid is supported by velocity anisotropy along the major axis. At this time, it has rotated clockwise less than $\sim 45°$ since formation; subsequently, its slow pattern speed declines even further as gravitational torques between the various components continue to transport angular momentum outward.

Around the central ellipsoid may be seen fainter loops and plumes of stars, most originating from intermediate radii in the incident disks. On the plot of $r$ against $v_r$ for the disk stars in Figure 9*b*, these loops show up as broad streams of circulating material, the most visible one turning around at $r \approx 1$. Similar but narrower streams may be seen in Figure 6 of Quinn's (1984) study of shell formation through accretion of relatively minor satellite galaxies. Stars once part of the tidal tails but not energetic enough to escape constitute the narrow stream falling back in from the right; their more energetic cohorts now populate the enormous tails shown in Figure 8*d*, which extend to $\sim 60$ times the scale length of the original exponential disks. These stars ride outward with the corresponding surge of dark material shown in Figure 9*c*; nearly all particles presently beyond $r \gtrsim 4.5$ will escape. The distribution function is obviously continuous through $E = 0$; hence, the density profile of the outer envelope will eventually tend to $\rho \propto r^{-4}$ as argued by Aguilar and White (1986).

Further information about the density structure of the remnant is presented in Figure 10, where cumulative mass profiles are shown for the bulge and disk, the total luminous component, and the dark halo. At smaller radii the bulge provides the dominant contribution, closely followed by the disk and halo; the luminous components dominate out to $r \approx 0.16$ length units. Comparing this plot with the corresponding figure for an initial galaxy, presented in Appendix B, it is clear that the merger has preserved a significant degree of segregation between the various components, but the halo and especially the disk have "mixed in" with the bulge at small radii.

Like the peculiar galaxy NGC 7252 studied by Schweizer (1982), the remnant described here exhibits various plumes and a pair of extended tidal tails, and like NGC 7252, the main body of the remnant is photometrically similar to an elliptical galaxy. This is illustrated in Figure 11, where the logarithm of the projected surface density of the luminous components is plotted as a function of radius to the one-fourth power; as usual, this transformation maps de Vaucouleurs law into a straight line. The surface density, measured with a circular aperture for simplicity, roughly follows an $r^{1/4}$ law all the way in to the scale where softening becomes important, which typi-

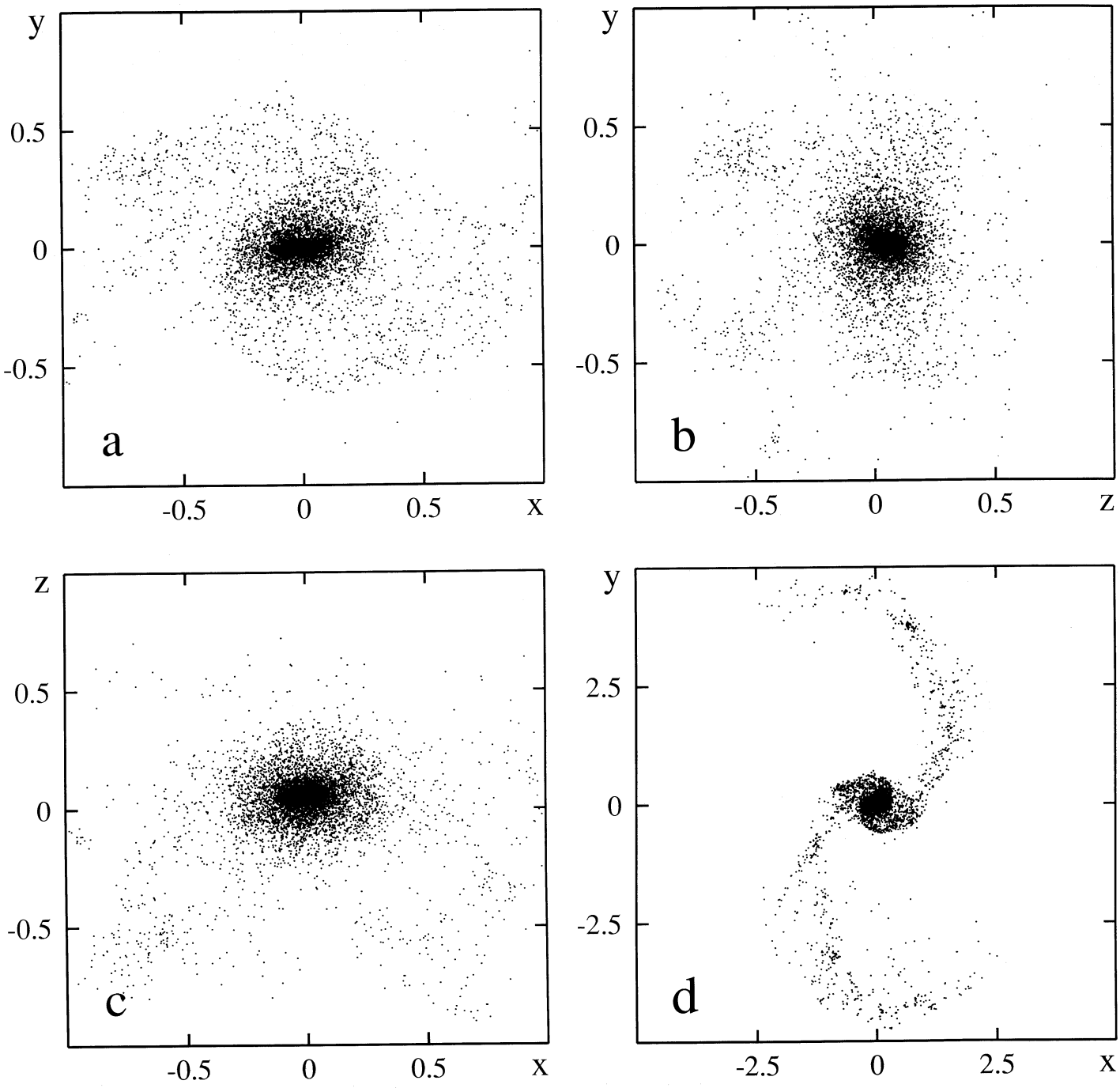


FIG. 8.—Merger remnant produced by encounter 1, sampled at $t = 4$. Looking down on the orbital plane, (*a*) is a closeup of the central object, while (*b*) and (*c*) are orthogonal projections edge-on to the orbital plane. (*d*) Large-scale view of the same projection as (*a*), showing the extended tidal tails.

cally corresponds to a few hundred parsecs. To be sure, several previous $N$-body studies claimed to reproduce White's (1979) original result that mergers generically produce de Vaucouleurs profiles, but it is encouraging to affirm it yet again. Still more encouraging is the smallish effective radius of the remnant, measured from Figure 11 to be $r_e \approx 0.1$. This is just slightly larger than the exponential scale length of the incident disks; hence if the infalling galaxies had been luminous spirals with scale length $\alpha^{-1} \approx 3.5$ kpc, the resulting elliptical would have an effective radius $r_e \approx 4$ kpc.

The high surface brightness of the remnant is a direct consequence of the fact that the *final* merger of the luminous components occurs from a subparabolic orbit; had the galaxies merged directly from a parabolic orbit, the characteristic surface brightness would have fallen by a factor of 2, instead of remaining roughly constant. Another consequence is that the velocity dispersion of bulge stars in the remnant turns out to be $\sim 1.4$ times the velocity dispersion of the incident bulges; if the bulges had merged directly, the expected ratio would have been unity. These corrections to the "homologous merger"

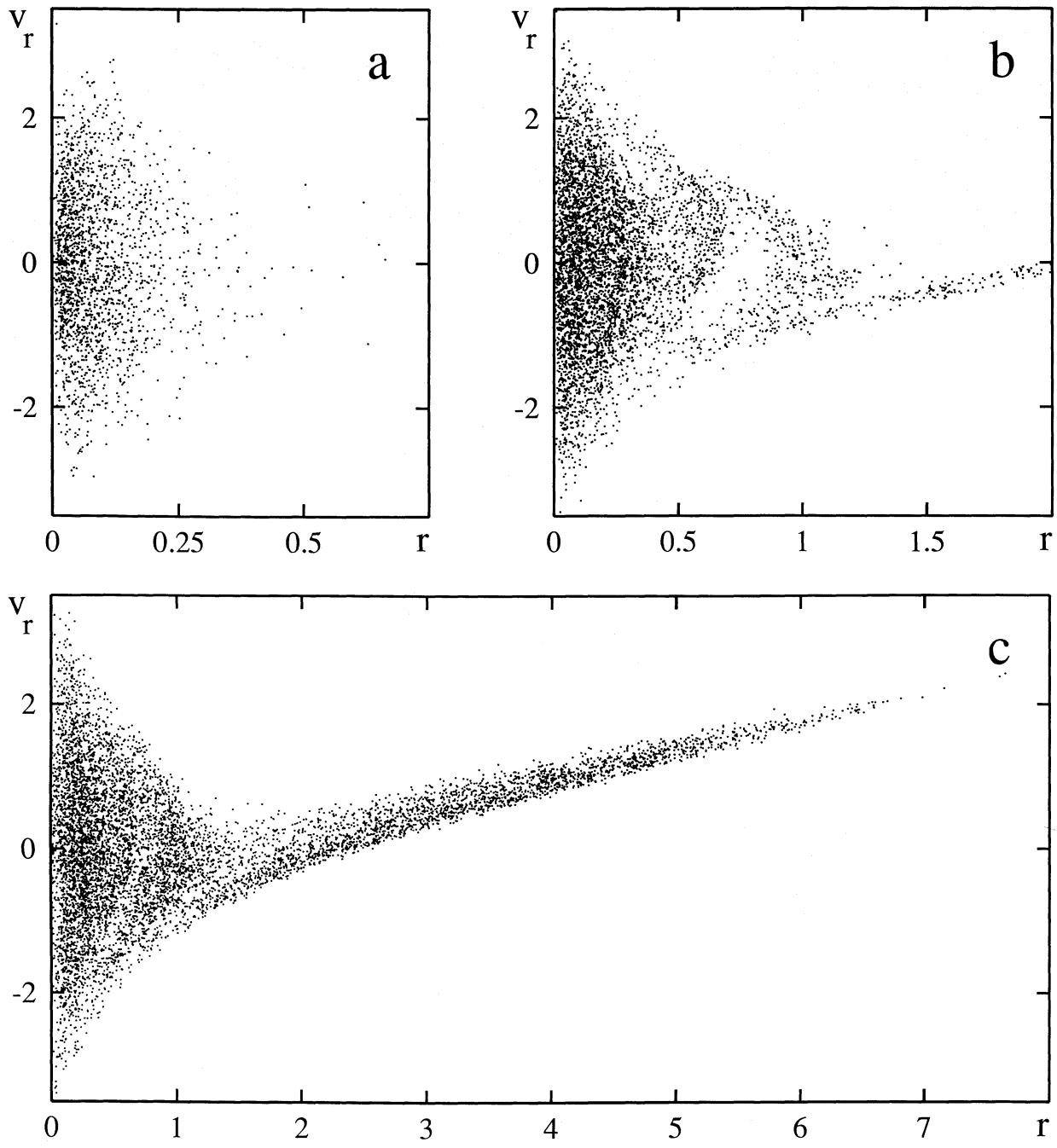


FIG. 9.—Phase space structure at $t = 4$ of the merger remnant produced by encounter 1. Radial velocity $v_r$ is plotted vs. radius $r$. Distribution of (*a*) bulge, (*b*) disk, and (*c*) halo components, respectively. Note the horizontal scale changes by a factor of 2 from each panel to the next.

prediction go a long way toward resolving the rather modest discrepancies between merger remnants and ellipticals reported by Veeraraghavan and White (1985).

## V. DISCUSSION AND CONCLUSIONS

As we have just seen, interacting disk/halo galaxies exhibit a wealth of interesting dynamics. These systems can be studied directly by self-consistent $N$-body techniques, but until now the costs of such simulations have discouraged realistic applications. With new $N$-body algorithms and increasing resources of computer time, the collision of disk galaxies is becoming a subject for detailed quantitative investigation instead of qualitative approximations.

The NGC 4038/9 look-alike presented in § II illustrates the kinds of calculations which are now possible, and it brings up some of the issues which arise when comparing a simulation to detailed observations. Subjectively, the model comes very close to matching the appearance of the Antennae, and this provides good grounds for confidence that the basic elements are correct. The self-consistent calculation confirms TT's hope that dynamical friction would remedy the implausibly large separation of the main bodies of the galaxies in their test particle

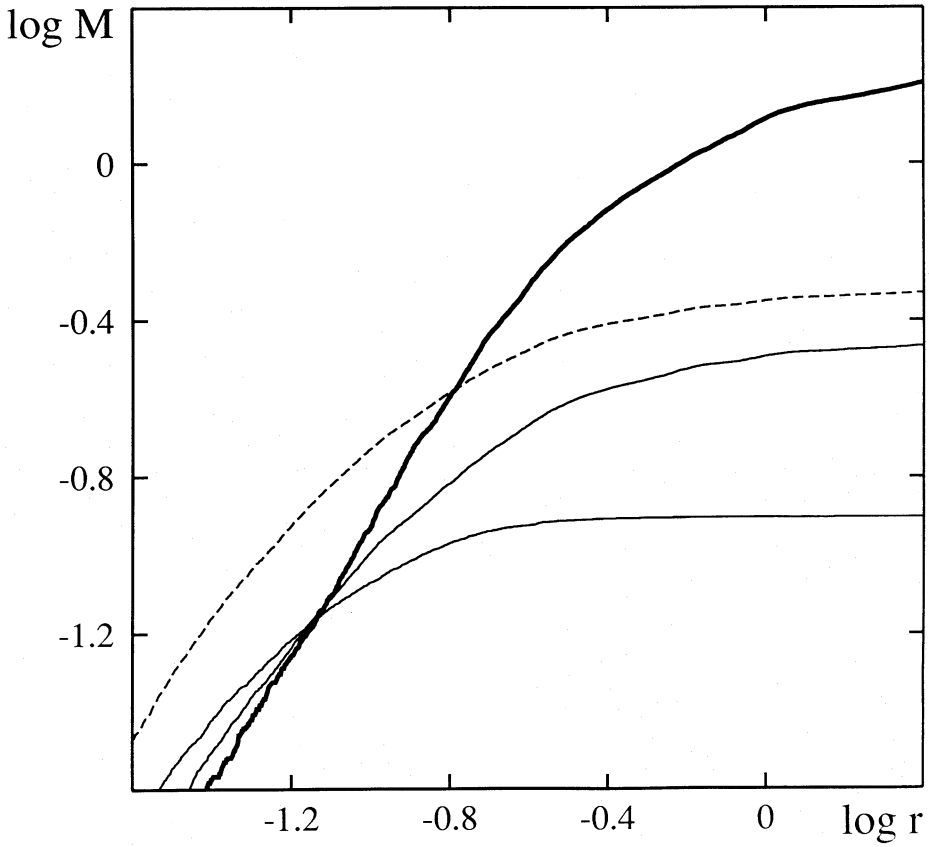


FIG. 10.—Cumulative mass profiles for the merger remnant. In order of increasing value at large $r$, profiles are shown for the bulge and disk, using thin lines, the total luminous component, using a dashed line, and the dark halo, using a thick line.

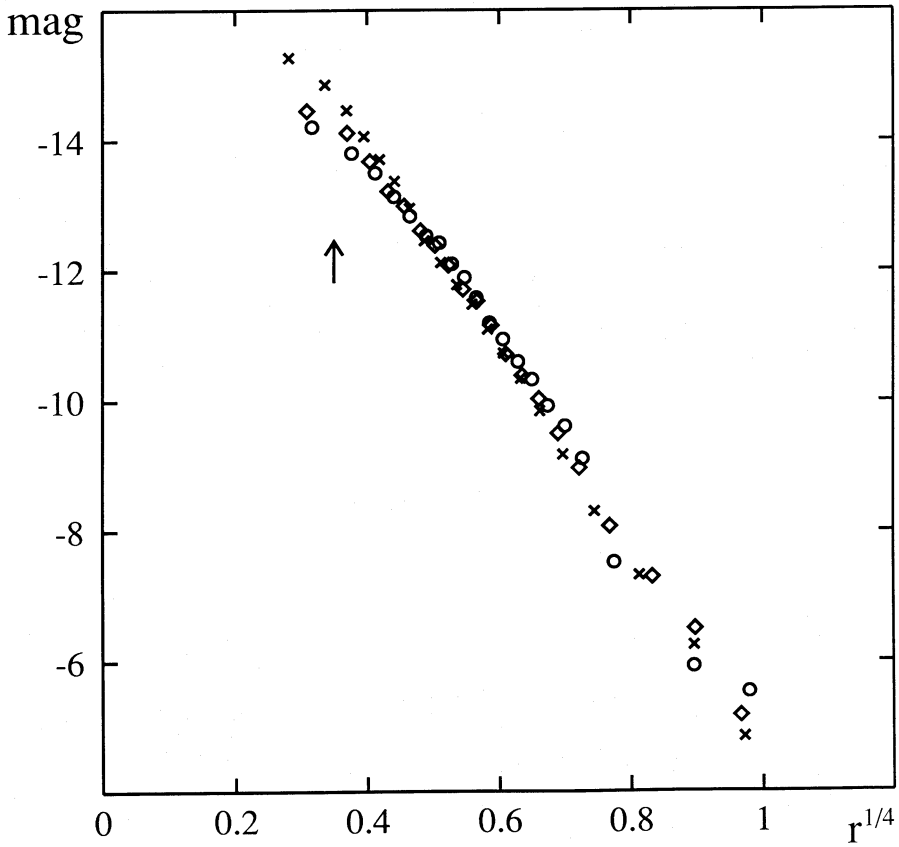


FIG. 11.—Surface density of luminous particles plotted against $r^{1/4}$, where "mag" is $-2.5$ log (surface density). Crosses, circles, and diamonds represent measurements made projecting the bulge and disk particles along the $x$, $y$, and $z$ directions, respectively. Arrow indicates the scale corresponding to the softening length.

model. Yet the verisimilitude of the model described here was also improved by a chance fluctuation which happened to grow to macroscopic proportions at the right time and place to produce asymmetric tails. Since fluctuations occur in real systems as well, we cannot expect to infer precise properties of the antecedent galaxies, nor to establish any given model as particularly unique.

Turning to more hypothetical situations, the simulations described in § III help answer several outstanding questions about interacting disk galaxies. First, they show that dynamical friction between two disk/halo galaxies can indeed provide the powerful braking necessary to merge the galaxies before the tails fly away. The connection between halos, merging and the formation of tidal tails seems to be rather subtle. Encounters involving galaxies with dark halos produce nice-looking tails from a variety of initial conditions; halos boost the effective encounter speeds of the disks, which respond self-consistently to a short but violent tidal perturbation by launching some small fraction of their mass with roughly escape velocity. Without dark halos, galaxies passing at the same distance suffer slower, more destructive encounters; dynamical friction between the disks can still bring them to a fairly rapid halt, but the resulting splash of disk mass does not look much like a pair of tidal tails. Increasing the impact parameter would reduce the overall splash, but the galaxies are then unlikely to merge soon enough. Dark halos are helpful and perhaps even *crucial* for raising thin, dynamically young tidal tails from closely interacting galaxies and merger remnants.

The collective response of the dark halos also plays a vital role in establishing the global parameters and gross properties of the remnants themselves. Halos provide a "sink" for binding energy and angular momentum as the visible galaxies spiral together; the final encounter of the most condensed luminous components always takes place from a much shrunken, tightly bound orbit. In these circumstances it is not surprising that the merger remnants are not homologous to their predecessors. Even without invoking gaseous dissipation, the surface brightness and velocity dispersions of the remnant described in § IV are dramatically higher than would be expected had the luminous galaxies merged directly without benefit of dark halos. This result is in happy agreement with a recent study of merger remnants by Lake and Dressler (1986), who found them to have significantly higher velocity dispersions than predicted from simple models of merger from near-parabolic encounters. The highly effective transport of angular momentum seen in encounter 1 and in other bulge/disk/halo galaxy mergers leaves slowly rotating remnants flattened by velocity anisotropy. These remnants are quite consistent with the slowly rotating bright elliptical galaxies first described by Bertola and Capaccioli (1975).

To be sure, all of these arguments need to be strengthened by much more work. While the comparison of encounters run with and without dark matter seems to favor the former, a careful reader might object that galaxy model 1, already contains perhaps twice as much dark matter as demanded by current "maximum disk" models, while model 0, with an almost Keplerian rotation curve, is something of a fake. To determine how much halo mass is really needed, many additional tests with plausible "minimum halo" models will be required. Even using the present models, a more extensive survey of different initial conditions should prove very helpful.

A basic conclusion of TT's work was that much of the morphology of interacting galaxies can be produced by purely stellar-dynamical encounters of disk galaxies. The present study shows that this conclusion remains valid even when the interacting galaxies are embedded in massive dark halos and their dynamical evolution is followed self-consistently. Gas-dynamics and star formation will doubtless modify the composition and structure of merger relics, especially near their centers, yet the present study indicates that *the global parameters and properties of ordinary ellipticals can be produced by essentially stellar-dynamical mergers of disk/halo galaxies.* Although this result was prefigured by previous numerical studies and by observations of recent mergers, the evidence presented here leaves little doubt that the connection between merger remnants and elliptical galaxies is worth pursuing in still greater detail.

It is a pleasure to thank A. Toomre for advice, encouragement, and comments on the manuscript, and P. Hut for these things plus his collaboration in developing the software used for this research. L. Hernquist implemented the tree code in FORTRAN, and P. Teuben helped establish a beachhead on the Cyber205. Numerical calculations were run at the JVNC under NAC-1300 and on SUN stations at the IAS. I acknowledge support from New Jersey High Technology grant No. 88-240090-2.

## APPENDIX A

## CONSTRUCTING BULGE/DISK/HALO MODELS

The galaxy models used as raw material in the present encounter simulations are multicomponent systems in stable dynamical equilibrium. Up to three components are present: (1) a central *bulge*, (2) a thin, rotating *disk*, and optionally (3) a spherical, extended *halo*. To construct a model disk galaxy, the following procedure was used:

1. *Build initial spheriod.*—Construct $N$-body models for the central bulge and outer dark halo, superpose them, and relax. In these experiments, $N$-body realizations of single-component King (1966) models were used for both components. A King model is completely specified by three parameters, such as total mass $M$, three-dimensional rms velocity dispersion $V$, and dimensionless central potential $W_0$. Two independently generated $N$-body models were superposed, producing a concentric two-component system somewhat out of dynamical equilibrium. After following the combined system for a few overall crossing times, a new dynamical equilibrium was reached, with relatively little radial mixing of the two components.

2. *Grow disk inside spheroid.*—While following the self-consistent evolution of the spheroid, slowly impose the gravitational field of a disk. Here an exponential surface density distribution with inverse scale length $\alpha$ and total mass $M_D$ was used for the disk. As the disk field slowly increased over $\sim 10$ initial crossing times, the spheroid responded adiabatically, contracting radially but

flattening very little. Once the disk field reached its final value, it was held steady for roughly five more crossing times to establish equilibrium again.

3. *Realize disk with particles.*—Lay down particles following the mass distribution of the disk imposed above, and assign circular and random velocities approximately consistent with equilibrium. The exponential surface density was used to pick in-plane radial coordinates $s = (x^2 + y^2)^{1/2}$, while the azimuthal angle $\phi$ was drawn uniformly from $0 - 2\pi$ and the vertical coordinate $z$ was drawn from a Gaussian with dispersion equal to the softening length $\epsilon$, which as a rule is roughly the *minimum* scale height set by soft self-gravitation. Velocities assigned to each particle were the sum of a circular motion $v_c(s)$ plus Gaussian random components in the radial, azimuthal, and vertical directions. Pressure support in the disk may be parametrized by Toomre's $Q$, which relates the radial dispersion $\sigma_s = 3.58Q\mu/\kappa$ to the surface density $\mu$ and epicyclic frequency $\kappa$; the azimuthal dispersion is $\sigma_\phi = 0.5\sigma_s\kappa/\omega$, where $\omega$ is the orbital frequency, and the vertical dispersion is $\sigma_z = 0.5\sigma_s$, roughly as in the solar neighborhood. The circular velocity profile $v_c(r)$ was corrected for pressure support using an approximate formula following Negroponte (1982).

Clearly, many elements of this procedure are rather ad hoc, although step 2 may in fact emulate the evolution of galactic halos as disks accumulate inside them (see Barnes 1987). Once further work in this field demands more sophisticated models, it may be worthwhile turning to Schwarzschild's (1979) approach to construct rotationally symmetric models with specified mass distributions.

## APPENDIX B

## TESTS OF BDH MODELS

Fundamental parameters for three model galaxies used in this study are listed in Table 2, in units such that $G = 1$. Model 1, to be used as the "standard", has bulge, disk, and halo components with mass raios of 1:3:16, implying that the halo has 4 times the total mass of the bulge and disk combined. Model 0 does away with the halo, but to prevent violent disk instabilities, its bulge-to-disk mass ratio had to be increased to 1:1. In model 2, on the other hand, the total mass of the halo was doubled, while other halo parameters were adjusted so as to obtain the same initial halo core radius and central density as model 1; this "extra-halo" model closely resembles the standard one at small and intermediate radii, but its halo extends roughly twice as far.

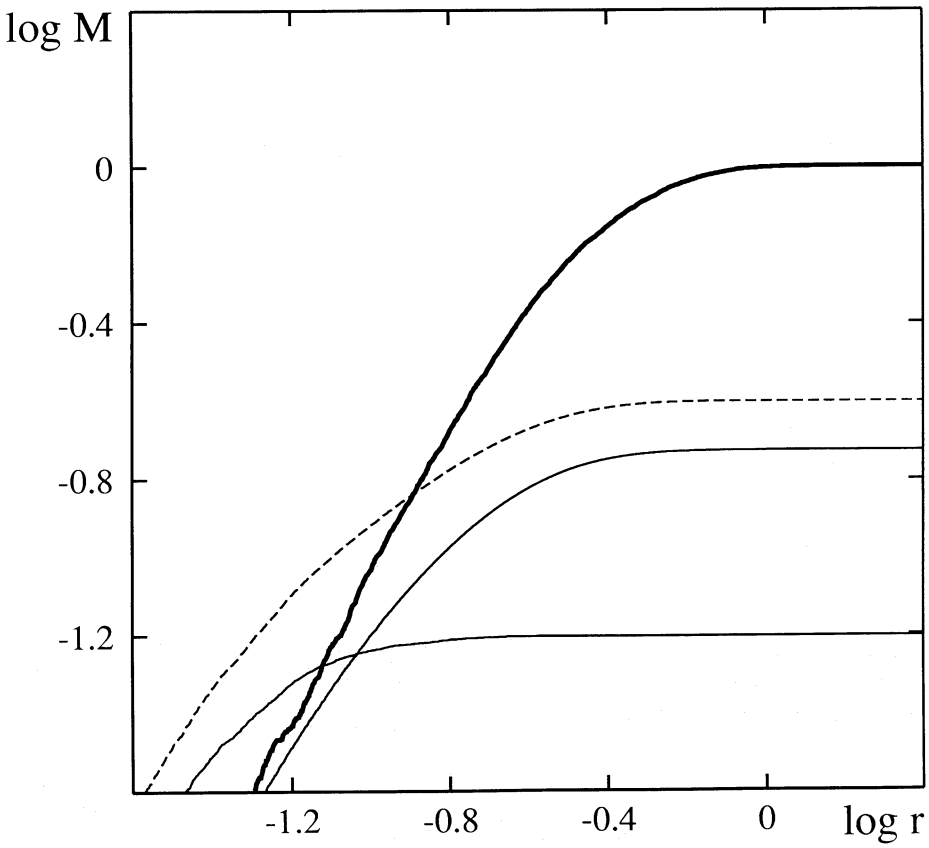


FIG. 12.—Cumulative mass profiles for galaxy model 1. In order of increasing value at large $r$, profiles are shown for the bulge and disk, the total luminous component, and the dark halo.

TABLE 2

MODEL GALAXIES[a]

| Identification | $W_{0B}$ | $M_B$ | $N_B$ | $M_D$ | $N_D$ | $W_{0H}$ | $M_H$ | $V_H$ | $N_H$ |
|---|---|---|---|---|---|---|---|---|---|
| 0..... | 5 | 1/8 | 2048 | 1/8 | 6144 | ... | ... | ... | ... |
| 1..... | 3 | 1/16 | 1024 | 3/16 | 3072 | 3 | 1 | 1 | 4096 |
| 2..... | 3 | 1/16 | 1024 | 3/16 | 3072 | 4.65 | 2 | 1.16 | 4096 |

NOTES.—The spheroidal components are generated from King 1966 models, which are completely specified by the dimensionless central potential $W_0$, total mass $M$, and three-dimensional velocity dispersion $V$; subscripts $B$ and $H$ apply to the bulge and halo, respectively. The disk follows an exponential surface density profile with a scale length of $1/\alpha$; the vertical scale height is set by $\epsilon$ as discussed in Appendix A; $Q$ is Toomre's parameter for local stability against axisymmetric perturbations. There are $N_B$, $N_D$, and $N_H$ particles in the bulge, disk, and halo, respectively.

[a] Common parameters: $V_B = 1$, $\alpha = 12.0$, $Q = 1.75$, $\varepsilon = 0.015$.

Since these models can be duplicated only by an elaborate constructive procedure, some details of their actual mass distributions follow. Figure 12 shows the cumulative mass profiles for the various components of model 1. Although the luminous components combine to dominate the mass at smaller radii ($r \lesssim 0.1$), the halo component dominates by a factor of $\sim 3$ within the nominal optical radius, $4.5/\alpha$. The extended halo produces a slowly rising and relatively featureless rotation curve. This is illustrated in Figure 13, where circular velocity curves for all three galaxy models are compared. The two halo models yield relatively plausible rotation curves, although both decline at large radii; to obtain truly level rotation curves, even more dark mass would have been required. In model 0 the rotation curve rises toward the center because so much of its mass is concentrated at small radii.

To check that these models are close to equilibrium and dynamical stability, tests were run using a C version of the Barnes and Hut (1986) tree code, setting the tolerance $\theta = 1$ and including quadrupole moments to get force calculations accurate to $\sim 10^{-2.5}$. A leapfrog integrator with time step $\Delta t = 1/128$ was used, together with a softening length $\epsilon = 0.015$. Each model was run for four time units, requiring $\sim 10$ days of CPU time on a Sun 3/50 with a f68881 coprocessor chip.

Face-on and edge-on views of model 1 at time $t = 1$ are shown in Figure 14. Since no sudden or violent rearrangement of the mass distribution occurs between $t = 0$ and 1, it appears that the initial conditions are fairly close to equilibrium, a conclusion supported,

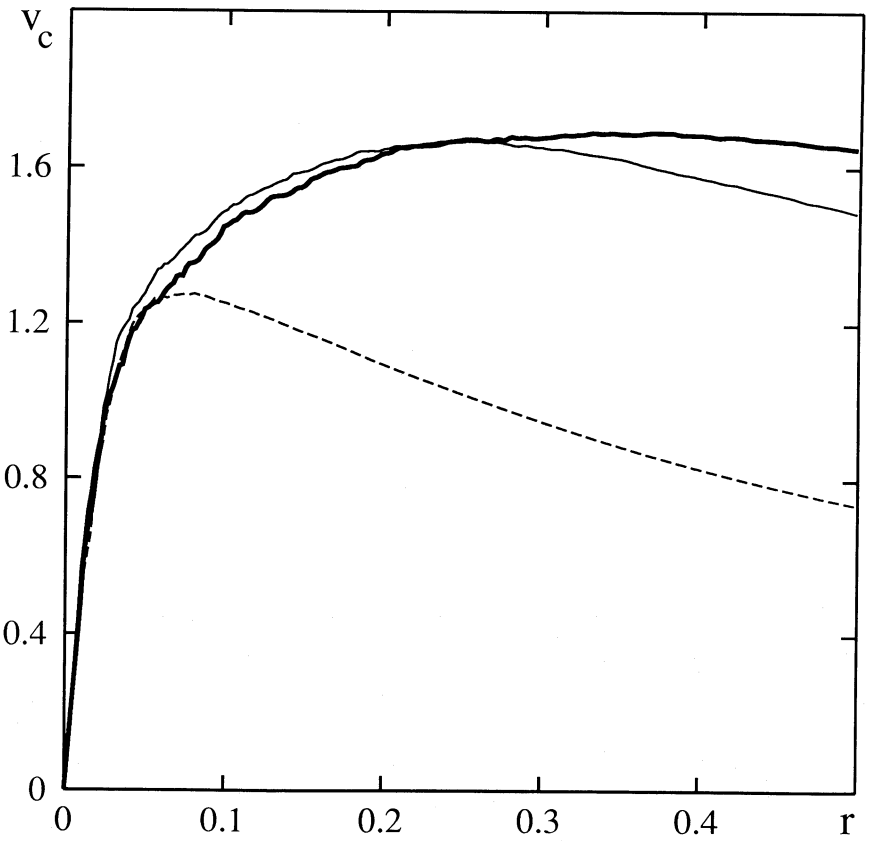


FIG. 13.—Circular velocity profiles ("rotation curves") for galaxy models 1, 2, and 0, plotted using thin, thick, and dashed lines, respectively

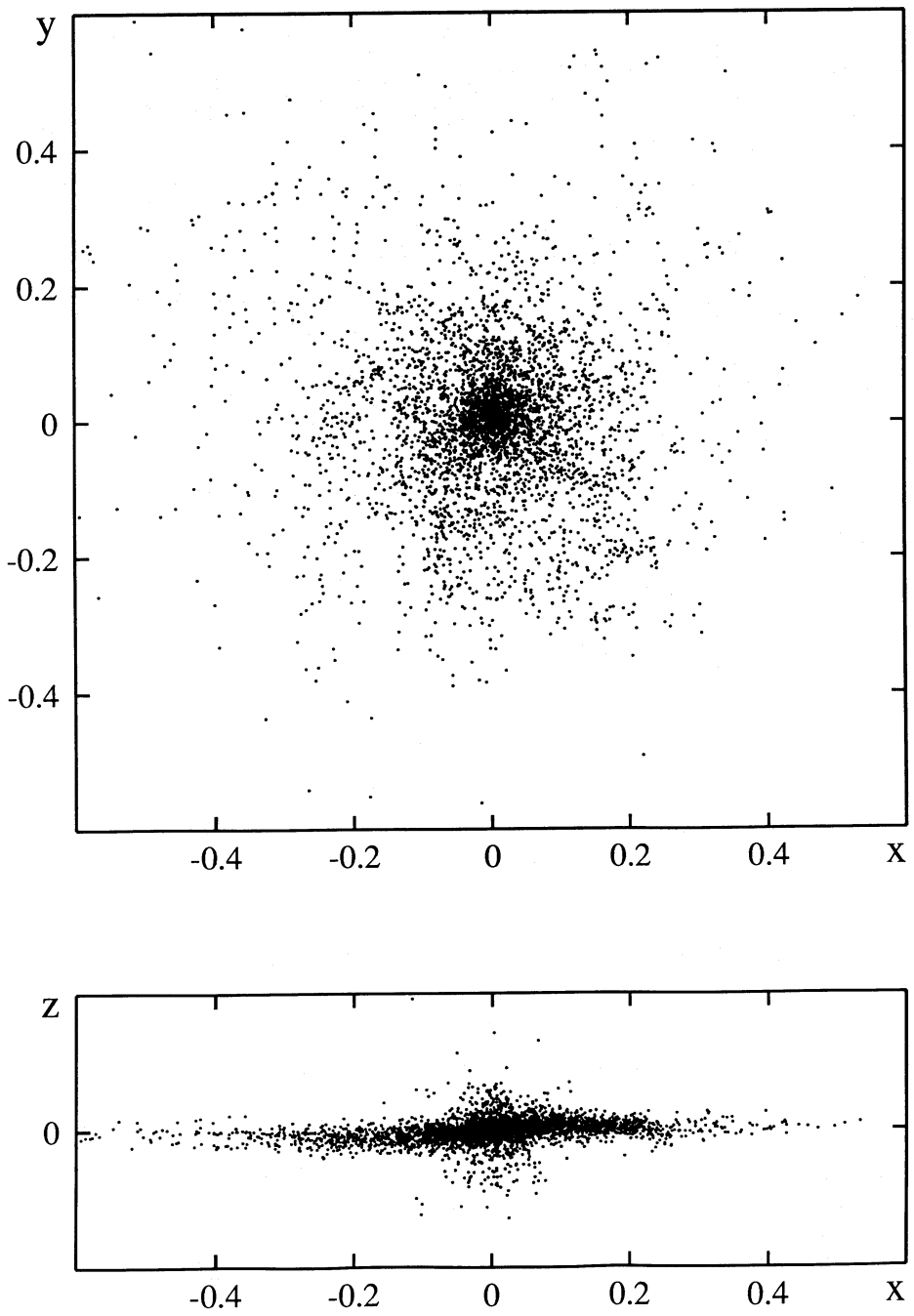


FIG. 14.—Face-on and edge-on snapshots of galaxy model 1 at $t = 1$ time units. Only luminous particles (bulge + disk) are plotted.

for instance, by examining the radial motion of disk particles over this time interval. On the other hand, this equilibrium is not completely stable, as shown by the development of shortlived spiral features visible face-on, and by the "flapping" and bending motions evident in the edge-on view. These transient fluctuations randomize particle velocities, steadily degrading the dynamical structure of the galaxy and especially the disk component. A rough measure of the damage may be obtained by computing the net vertical and inplane radial velocity dispersions of the disk component, $\sigma_z$ and $\sigma_s$. These quantities are plotted as functions of time $t$ for all three galaxy models in Figure 15. Model 0 evolves most slowly, probably because twice as many particles are used in the disk, until $t > 3$, at which time a bar begins to form and rapidly increases the radial velocity dispersion. Model 2 degrades fastest, perhaps because the relatively massive halo particles used in this case continually bombard the disk. The secular evolution of these models is clearly undesirable for interacting galaxy calculations, but it appears to be slow enough that interesting encounters can already be simulated before the disks degrade too much.

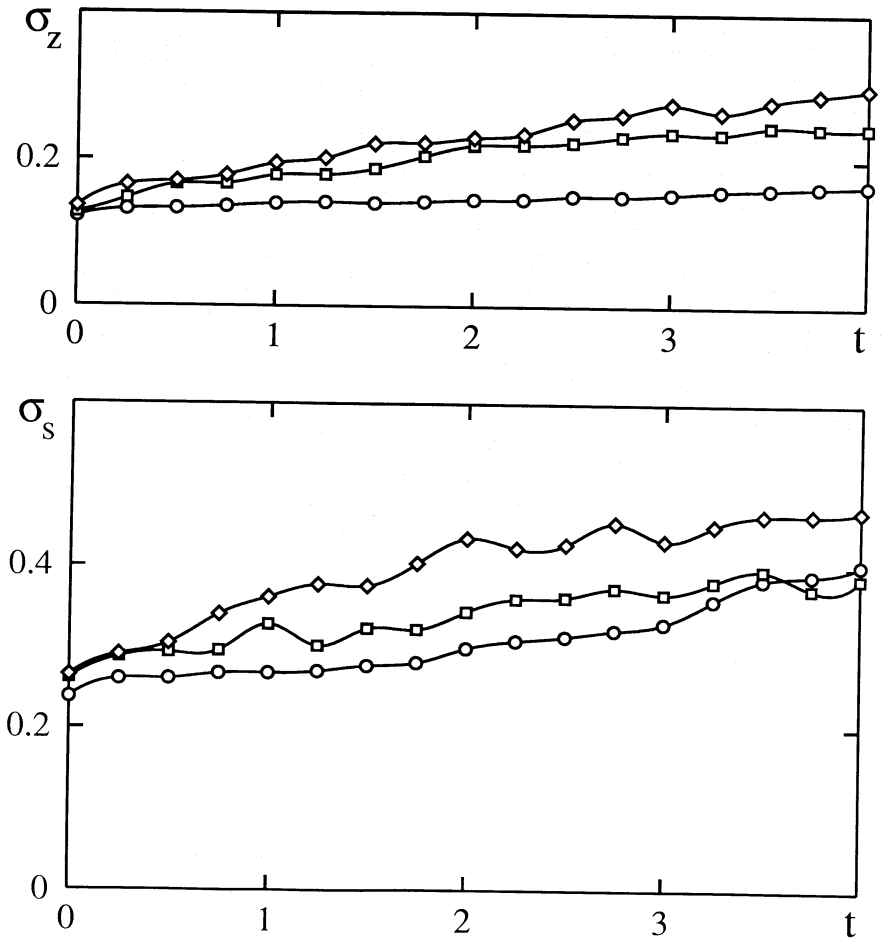


FIG. 15.—Stability of the three galaxy models as measured by the heating of the disk stars in the radial and vertical directions. Net radial and vertical dispersions $\sigma_s$ and $\sigma_z$ are plotted as functions of time, using circles, squares, and diamonds for models 0, 1, and 2, respectively.

## APPENDIX C

## CONSTRUCTING INITIAL CONDITIONS

Initial conditions for these encounter calculations were generated by launching a pair of equilibrium galaxy models at each other; that is, two independent BDH models were generated, placed near each other, and given a net relative motion leading to a close encounter. Strictly speaking, this prescription yielded somewhat artificial initial data, inasmuch as two equilibrium objects were simply juxtaposed in a nonequilibrium situation. More plausible initial conditions might have exhibited a gradual transition from equilibrium within the optical portions of the galaxies, where the crossing time is short, to nonequilibrium infall at large radii, where the crossing time is roughly the age of the universe. Systems with such a transition can be generated in cosmological $N$-body models, but the complications involved in "extracting" a pair of interacting halos from the model and inserting the appropriate bulge and disk components are so formidable as to deter this line of research.

Contrary to frequent $N$-body practice, these galaxy models were not first evolved in isolation to "relax" initial fluctuations; as seen in Appendix B, such relaxation would have had the effect of steadily degrading the dynamical structure of the disks, heating and thickening them in a few orbital times beyond what is observed in real galaxies. The unrelaxed disks, warts and all, should yield more realistic results for the interaction of actual galaxies, many of which probably have disks colder than $Q \approx 1.8$. For the same reason, and so as not to waste computer time, the present models were released from relatively close proximity, with outer halos almost touching.

The initial relative velocity of the two galaxies was prescribed from the Keplerian orbit of two corresponding point masses. Each galaxy was replaced by a point of the same mass, and a two-body orbit with eccentricity $e$ and pericentric distance $r_p$ was set up. The orbital phase was determined from the time until pericenter $t_p$ for the idealized orbit, and the orientation was chosen so that the two galaxies orbit clockwise in the $xy$-plane. Inasmuch as the major mass concentrations are roughly spherical and initially disjoint, this Keplerian orbit is asymptotically consistent, and the bulges of the galaxies typically followed the specified trajectory up to $\sim t_p$. With respect to the orbital plane, two angles are required to specify the orientation of each axisymmetric galaxy: like TT's Figure 6*a*, this study uses the inclination $i$, which is the angle between the spin plane and the separation vector at pericenter, measured in the orbit plane.

REFERENCES


Aguilar, L., and White, S. D. M. 1985, *Ap. J.*, **295**, 374.
———. 1986, *Ap. J.*, **307**, 97.
Arp, H. 1966, *Ap. J. Suppl.*, **14**, 1.
Barnes, J. 1987, in *Nearly Normal Galaxies: From the Planck Time to the Present*, ed. S. M. Faber (New York: Springer), p. 154.
Barnes, J., and Hut, P. 1986, *Nature*, **324**, 446.
———. 1988, in preparation.
Bertola, F., and Capaccioli, M. 1975, *Ap. J.*, **200**, 439.
Carlberg, R. G. 1986, *Ap. J.*, **310**, 593.
Eneev, T. M., Kozlov, N. N., and Sunyaev, R. A. 1973, *Astr. Ap.*, **28**, 41.
Faber, S., and Gallagher, J. 1979, *Ann. Rev. Astr. Ap.*, **17**, 135.
Farouki, R., and Shapiro, S. L. 1981, *Ap. J.*, **243**, 32.
Farouki, R., Shapiro, S. L., and Duncan, M. J. 1983, *Ap. J.*, **265**, 597.
Gerhard, O. 1981, *M.N.R.A.S.*, **197**, 179.
Hernquist, L. 1987, *Ap. J. Suppl.*, **64**, 715.
Hut, P., and Sussman, G. J. 1987, *Sci. Am.*, **257**, No. 4, 144.
King, I. 1966, *A.J.*, **76**, 64.
Lake, G., and Dressler, A. 1986, *Ap. J.*, **310**, 605.
Mahoney, J. H., van der Hulst, J. M., and Burke, B. F. 1987, preprint.
Miller, R., and Smith, B. 1980, *Ap. J.*, **235**, 421.
Negroponte, J. 1982, Ph.D. thesis, University of California.
Negroponte, J., and White, S. D. M. 1983, *M.N.R.A.S.*, **205**, 1009.
Noguchi, M. 1987, *M.N.R.A.S.*, **228**, 635.
Ostriker, J. P. 1980, *Comments Ap.*, **8**, 177.
Palmer, P. L., and Papaloizou, J. 1982, *M.N.R.A.S.*, **199**, 169.
Quinn, P. 1982, Ph.D. thesis, Australian National University.
———. 1984, *Ap. J.*, **279**, 596.
Rubin, V., Ford, K., and D'Odorico., S. 1970, *Ap. J.*, **160**, 801.
Schwarzschild, M. 1979, *Ap. J.*, **232**, 236.
Schweizer, F. 1978, in *Structure and Properties of Nearby Galaxies*, ed. E. M. Berkhuijsen and R. Wielebinski (Dordrecht: Reidel), p. 279.
———. 1982, *Ap. J.*, **252**, 455.
Toomre, A. 1977, in *The Evolution of Galaxies and Stellar Populations*, ed. B. M. Tinsley and R. B. Larson (New Haven: Yale Univ. Obs.), p. 401.
———. 1981, in *The Structure and Evolution of Normal Galaxies*, ed. S. M. Fall and D. Lynden-Bell (Cambridge: Cambridge University Press.), p. 111.
Toomre, A., and Toomre, J. 1972, *Ap. J.*, **179**, 623.
van Albada, T., and von Gorkom, J. 1977, *Astr. Ap.*, **54**, 121.
Veeraraghavan, S., and White, S. D. M. 1985, *Ap. J.*, **296**, 336.
Villumsen, J. 1982, *M.N.R.A.S.*, **199**, 493.
White, S. D. M. 1978, *M.N.R.A.S.*, **184**, 185.
———. 1979, *M.N.R.A.S.*, **189**, 831.
———. 1980, *M.N.R.A.S.*, **191**, 1P.
———. 1982, in *The Morphology and Dynamics of Galaxies*, ed. L. Martinet and M. Mayor (Sauverny: Geneva Obs.), p. 289.
White, S. D. M., and Rees, M. J. 1978, *M.N.R.A.S.*, **183**, 341.
Wright, A. E. 1972, *M.N.R.A.S.*, **157**, 309.
Zwicky, F. 1959, in *Handbuch der Physik*, Vol. **53**, ed. S. Flügge (New York: Springer), p. 373.


JOSHUA BARNES: Fuld Hall, Institute for Advanced Study, Olden Lane, Princeton, NJ 08540